10.1515/tvsb-2015-0013

Transactions of the VŠB – Technical University of Ostrava

Civil Engineering Series, No. 2, Vol. 15, 2015

paper #13

Juraj KRÁLIK[1], Oľga HUBOVÁ[2], Lenka KONEČNÁ[3]

CFD SIMULATION OF AIR-FLOW OVER A „QUARTER-CIRCULAR" OBJECT VALIDED BY EXPERIMENTAL MEASUREMENT

Abstract

A Computer-Fluid-Dynamic (CFD) simulation of air-flow around quarter-circular object using commercial software ANSYS Fluent was used to study iteration of building to air-flow. Several, well know transient turbulence models were used and results were compared to experimental measurement of this object in Boundary Layer Wind Tunnel (BLWT) of Slovak University of Technology (SUT) in Bratislava. Main focus of this article is to compare pressure values from CFD in three different elevations, which were obtained from experimental measurement. Polyhedral mesh type was used in the simulation. Best results on the windward face elevations were obtained using LES turbulence model, where the averaged difference was around 7.71 %. On the leeward face elevations it was SAS turbulence model and averaged differences from was 15.91 %. On the circular face it was SAS turbulence model and averaged differences from all elevations was 12.93 %.

Keywords

ANSYS, CFD, turbulence, pressure, experiment.

1 INTRODUCTION

A useful tool to study building to air-flow iteration is Computer Fluid Dynamics (CFD). CFD is widely used by engineers and designers to predict air-flows and influence turbulence. Accuracy of simulations depends on problem statement and choosing the right turbulence model with corresponding grid sensitivity. The flow fields are characterized by the presence of multiple recirculation zones embedded within a unidirectional flow.

In this paper are CFD simulations of air-flow over an obstacle in shape of quarter-circular object is presented and compared to data from experimental measurement. For the needs of simulation, two models were created with different grid sensitivity. Polyhedral mesh type was used to create a domain with low computer demands.

2 TURBULENCE MODELLING

Modelling of turbulence or air flow around an obstacle can be done by many commercial and non-commercial programs. For purpose of this article was used Fluent R15 which is part of ANSYS commercial package. Fluent offers many turbulence models, from one equation up to seven equation turbulence model. In this analysis were used following turbulence models: k-ε (2-eq. model); k-ω (2-

[1] Ing. Juraj Králik, Ph.D., Institute of Construction in Architecture and Engineering Structures, Faculty of Architecture, Slovak University of Technology in Bratislava, Námestie Slobody 19, 812 45 Bratislava, Slovakia, phone: (+421) 903 951 403, e-mail: kralik@fa.stuba.sk.

[2] Doc. Ing. Oľga Hubová, Ph.D., Department of Structural Mechanics, Faculty of Civil Engineering, Slovak University of Technology in Bratislava, Radlinského 11, 810 05 Bratislava, Slovakia, e-mail: olga.hubova@stuba.sk.

[3] Ing. Lenka Konečná, Ph.D., Department of Structural Mechanics, Faculty of Civil Engineering, Slovak University of Technology in Bratislava, Radlinského 11, 810 05 Bratislava, Slovakia, e-mail: lenka.konecna@stuba.sk.

eq. model); SST (Shear-Stress Transport, 4-eq. model); SAS (Scale-Adaptive Simulation) and LES (Large Eddy Simulation). All these turbulence models are well described in ANSYS manuals, so next will follow only a brief description of these models and for comparison of models their model formulation will be presented theirs differential transport equations.

2.1 *k-ε* model

This model is valid for fully turbulent flows only. Widely used despite the known limitations of the model. Performs poorly for complex flows involving severe pressure gradients, separations and strong streamline curvature. Fluent offers three variants of this turbulence model: Standard, RNG and Realizable and four types of near-wall modelling: standard wall functions, scalable wall functions, non-equilibrium wall functions, enhanced wall treatment and user defined wall functions. Differential transport equations for the turbulence kinetic energy and turbulence dissipation rate [1]:

$$\frac{\partial(\rho k)}{\partial t}+\frac{\partial(\rho U_j k)}{\partial x_j}=P_k-\rho\varepsilon+P_{kb}+\frac{\partial}{\partial x_j}\left[\left(\mu+\frac{\mu_t}{\sigma_k}\right)\frac{\partial k}{\partial x_j}\right] \quad (1)$$

$$\frac{\partial(\rho\varepsilon)}{\partial t}+\frac{\partial(\rho U_j\varepsilon)}{\partial x_j}=\frac{\varepsilon}{k}(C_{\varepsilon1}P_k-C_{\varepsilon2}\rho\varepsilon+C_{\varepsilon1}P_{\varepsilon b})+\frac{\partial}{\partial x_j}\left[\left(\mu+\frac{\mu_t}{\sigma_\varepsilon}\right)\frac{\partial k}{\partial x_j}\right] \quad (2)$$

2.2 *k-ω* model

Superior performance for wall-bounded boundary layer, free shear, and low Reynolds number flows. Suitable for complex boundary layer flows under adverse pressure gradient and separation (external aerodynamics and turbomachinery). Can be used for transitional flows (though tends to predict early transition). Separation is typically predicted to be excessive and early. Fluent offers two variants of this turbulence model: Standard and SST. Model formulation for turbulent kinetic energy and turbulent frequency [2,3]:

$$\frac{\partial(\rho k)}{\partial t}+\frac{\partial(\rho U_j k)}{\partial x_j}=P_k-\beta^*\rho k\omega+P_{kb}+\frac{\partial}{\partial x_j}\left[\left(\mu+\frac{\mu_t}{\sigma_\omega}\right)\frac{\partial k}{\partial x_j}\right] \quad (3)$$

$$\frac{\partial(\rho\omega)}{\partial t}+\frac{\partial(\rho U_j\omega)}{\partial x_j}=\alpha\frac{\omega}{k}P_k-\beta\rho\omega^2+P_{\omega b}+\frac{\partial}{\partial x_j}\left[\left(\mu+\frac{\mu_t}{\sigma_\omega}\right)\frac{\partial k}{\partial x_j}\right] \quad (4)$$

2.3 Shear-Stress Transport

These models can simulate the laminar-turbulent transition of wall boundary layers. Proper mesh refinement and specification of inlet turbulence levels is crucial for accurate transition prediction. In general, there is some additional effort required during the mesh generation phase because a low-Re mesh with sufficient stream-wise resolution is needed to accurately resolve the transition region. Fluent offers two variants of scale-resolving simulation options: scale-adaptive simulation and detached eddy simulation. SST model formulation [4,5]:

$$\frac{\partial(\rho k)}{\partial t}+\frac{\partial(\rho U_i k)}{\partial x_i}=\tilde{P}_k-\beta^*\rho k\omega+\frac{\partial}{\partial x_i}\left[(\mu+\sigma_k\mu_t)\frac{\partial k}{\partial x_i}\right] \quad (5)$$

The turbulent eddy viscosity is defined as follows:

$$v_t=\frac{a_1 k}{max(a_1\omega,SF_2)} \quad \rightarrow \quad v_t=\frac{\mu_t}{\rho} \quad (6)$$

2.4 Scale-Adaptive Simulation

The full transition model is based on two transport equations, one for the intermittency and one for the transition onset criteria in terms of momentum thickness Reynolds number. It is called ‘Gamma Theta Model’ and is the recommended transition model for general-purpose applications. It uses a new empirical correlation (Langtry and Menter) which has been developed to cover standard bypass transition as well as flows in low free-stream turbulence environments. Used for globally unstable flows, ‘safest’ SRS model, as it has URANS fall-back position on coarse grids/time steps, [6, 7 and 8]. The transport equation for the intermittency and for the transition momentum thickness Reynolds number:

$$\frac{\partial(\rho\gamma)}{\partial t}+\frac{\partial(\rho U_j\gamma)}{\partial x_j}=P_{\gamma 1}-E_{\gamma 1}+P_{\gamma 2}-E_{\gamma 2}+\frac{\partial}{\partial x_j}\left[\left(\mu+\frac{\mu_t}{\sigma_\gamma}\right)\frac{\partial\gamma}{\partial x_j}\right] \quad (7)$$

2.5 Large Eddy Simulation

Turbulent flows are characterized by eddies with a wide range of length and time scales. The largest eddies are typically comparable in size to the characteristic length of the mean flow. The smallest scales are responsible for the dissipation of turbulence kinetic energy. Used for free shear flows, typically too expensive for wall-bounded flows. Fluent offers five variants of this turbulence model: Smagorinsky-Lilly, WALE, WMLES, WMLES S-Omega and Kinetic-Energy Transport. In the WALE model [9], the eddy viscosity is modelled by:

$$\mu_t=\rho L_S^2\frac{\left(S_{ij}^d S_{ij}^d\right)^{3/2}}{\left(\bar{S}_{ij}\bar{S}_{ij}\right)^{5/2}+\left(S_{ij}^d S_{ij}^d\right)^{5/4}} \quad (9)$$

3 EXPERIMENT

Experimental measurement was carry out in Boundary Layer Wind Tunnel (BLWT) of Slovak University of Technology in Bratislava, Fig.1. Examined object was quarter-circle shape that was 273 mm high and the quarter-circle radius was 80 mm with 30 mm rectangle part at the ends of quarter-circle. During this experiment were measured pressures in 16 points in three different elevations 15, 136 and 258 mm above the wind tunnel floor level, Fig.1. During experiment was from previous measurements found out that the most unpleasant direction of wind was when the model was rotated by approximately 112° from its original position (when wind direction was perpendicular to the one of the rectangle face of the model), [10].

Three sets of data were obtained for each elevation, for model rotated by 120°. Every set of data consisted of approximately 500 values of pressure in each measuring point. For comparison to CFD simulations were calculated three curves of pressures in each elevation: max., min. and mean.

Measurement conditions were as follows: the frequency of rotors was 20 Hz; the barometric pressure was varying from 100 440 Pa up to 100 460 Pa; the air density 1.18843 kg/m^3 up to 1.18947 kg/m^3 and the air temperature 19.8°C up to 21°C. Reference value of wind speed were measured 369 mm in front of the model in the high of top edge of object (273 mm) and were as follows: 8.92 m/s; 8.85 m/s; 8.42 m/s and 8.49 m/s. Mean value of reference wind speed was interpolated to 8.745 m/s.

Fig. 1: Left: STU BLWT; Right: model

It needs to be noted that during this experiment wasn't measured wind profile for the frequency of rotors (20 Hz). The data for wind profile used in CFD simulation were taken from previous measurements in BLWT for the frequency of rotors 18 Hz and 26 Hz. Subsequently the data for wind profile for frequency of 20 Hz were interpolated and the wind profile can be seen in Fig.2 (black coloured curve).

4 COMPUTER-FLUID-DYNAMIC

As mention before for purpose of this analyse was used ANSYS Fluent R15 software.

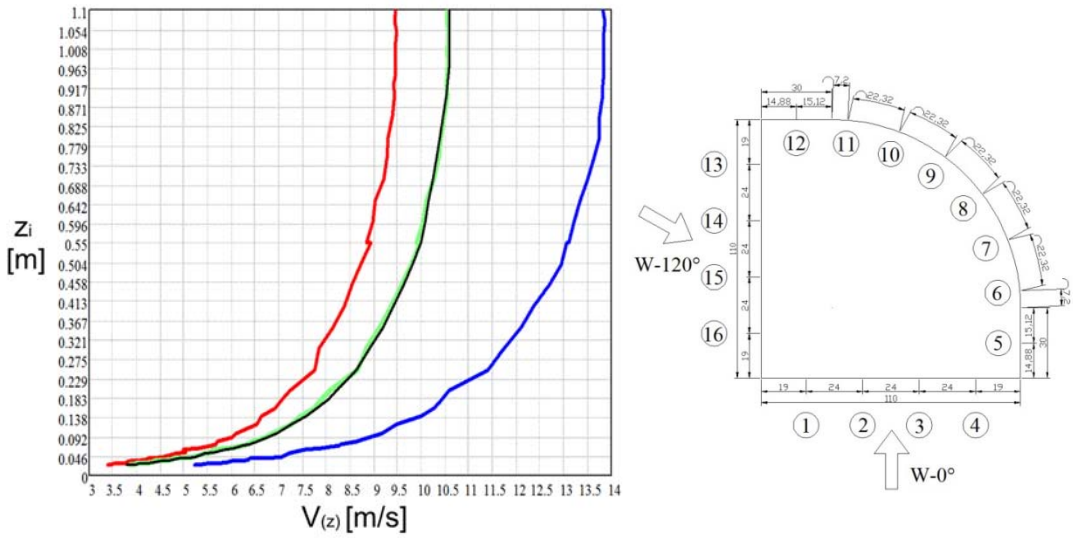

Fig. 2: Left: wind profiles: 18 Hz (red); 26 Hz (blue); 20 Hz (green) and CFD profile (black); Right: location of pressure taps with respect to wind direction

4.1 Geometry

Geometry was built in Design Modeller. Whole grid dimensions are: L=4 m, B=2.6 m and H=1.6 m. Quarter-circle object was situated 1m behind inlet boundary (his centre of gravity) in middle of domains width.

4.2 Mesh

Original mesh was generated using tetrahedron elements and two types of mesh where created. First mesh had on surface of quarter-circle object element size 0.005 m, advanced size function was on and set to be fixed, with fine relevance centre, high smoothing and slow transition. Maximum face size was 0.1 m, maximum size 0.2 m and grow rate of elements from surface of object 5%. Generated were $1.8 \cdot 10^6$ elements with 341 504 nodes, model mark is M1. Second mesh had on surface of quarter-circle object element size 0.003 m, advanced size function was on and set to be fixed, with fine relevance centre, high smoothing and slow transition. Maximum face size was 0.1 m, maximum size 0.2 m and grow rate of elements from surface of object 5%. Generated were $3.347 \cdot 10^6$ elements with 663 398 nodes, model mark is M2. Both types of mesh were converted in ICEM (fluent solution module) to polyhedral mesh type with final element number for first mesh 354593 polyhedral cells with 2088288 nodes, second had 700200 polyhedral cells with 3448831 nodes.

4.3 Boundary layers

Each surface had to have its “named section” to which were in solution module set boundary condition. Inlet was set as velocity inlet, outlet as outflow and rest of faces was set as no slip walls without roughness.

4.4 Inputs

In this analysis were used several turbulence models, where each of these models needed his specific inputs. For all models was used same wind velocity profile, which was defined as user defined function (UDF) and interpreted to ICEM. Wind profile was divided into five zones, in the parts where

used classic logarithmic function split away from wind profile for the 20 Hz frequency of rotors. These heights were 70 mm, 250 mm, 550 mm and 950 mm from where the velocity was almost constant.

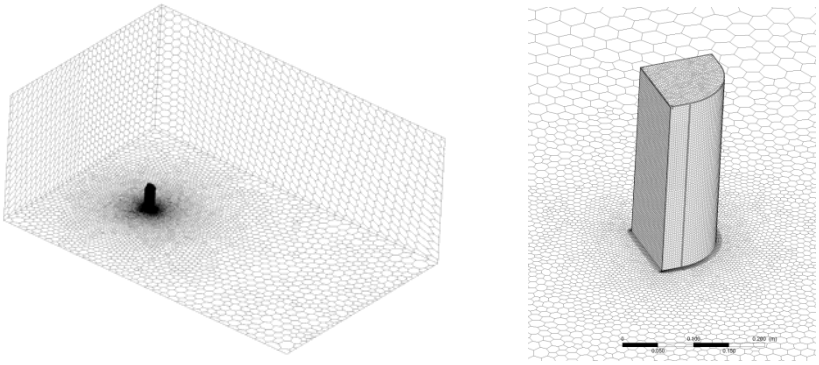

Fig. 3: Model mesh view

Used logarithmic function was:

$$U(z) = u_{z_0} \cdot A_1 + \frac{u_{fric}}{B_1} \cdot ln\left(\frac{z}{C_1 z_0}\right) \tag{10}$$

Upper constant part of velocity profile was:

$$U(z) = u_{z_0} \cdot A_1 + \frac{u_{fric}}{B_1} \cdot ln\left(\frac{z}{C_1 z_0}\right) + \frac{z}{50} \tag{11}$$

Where u_{z0}=3.851 m/s was speed at height of terrain roughness z_0=0.02 m (nops foil height). Friction wind velocity was defined as:

$$u_{fric} = \frac{u_{ref} - u_{z_0}}{ln\left(\frac{z_{ref}+50 \cdot z_0}{4 \cdot z_0}\right)} = \frac{8.745-3.851}{ln\left(\frac{0.273+50 \cdot 0.02}{4 \cdot 0.02}\right)} = 1.67\ m/s \tag{12}$$

Wind profile constants were as follows: A=(0.81; 1; 1.031; 1.65), B=(0.7; 0.9; 0.935; 1.55), C=0.95. Comparison of final UDF wind velocity profile to interpolated wind velocity profile can be seen on Fig.2. it need to be noted that the logarithmic function and constants were set to obtain wind velocity profile as much as it is possible the same as was interpolated profile, error in wind velocity at reference height (z_{ref}=0.273 m) was zero, maximum error through the whole curve was 4.3%.

k-ε model: this model inputs are based on turbulent kinetic energy *k* and turbulence dissipation rate *ε* as follows:

$$u = \frac{u_{ref} \cdot \kappa}{ln\left(\frac{z_{ref}}{z_0}\right)} = \frac{8.745 \cdot 0.4}{ln\left(\frac{0.273}{0.02}\right)} = 1.338\ m/s \tag{13}$$

$$k = \frac{u^2}{\sqrt{C_\mu}} = \frac{1.338^2}{\sqrt{0.09}} = 5.97\ m^2/s^2 \tag{14}$$

$$\varepsilon(z) = \frac{u^3}{\kappa \cdot (z+z_0)} \tag{15}$$

k-ω model: this model inputs are based on turbulent kinetic energy *k* and specific turbulence dissipation rate *ω* as follows:

$$\omega(z) = \frac{\varepsilon(z)}{k} \tag{16}$$

SST model: this model inputs are based on intermittency *γ* (0~1), turbulent kinetic energy *k* and specific turbulence dissipation rate *ω*.

SAS model: this model inputs are based on turbulent kinetic energy *k* and specific turbulence dissipation rate *ω*.

LES model: this model inputs are based on turbulent kinetic energy k and turbulence dissipation rate ε.

Absolute convergence criteria were set for residual to 10^{-4}. Spectral synthesiser was used to simulate fully turbulent environment (SRS turbulence models).

5 RESULTS

During experiment were measured only values of pressure in selected points in three different elevations, so results are focused on comparison of mean values of pressures obtained from transient simulations, which are compared to values of pressures from experiment measurements. On the following graphs are represented results from several transient simulations.

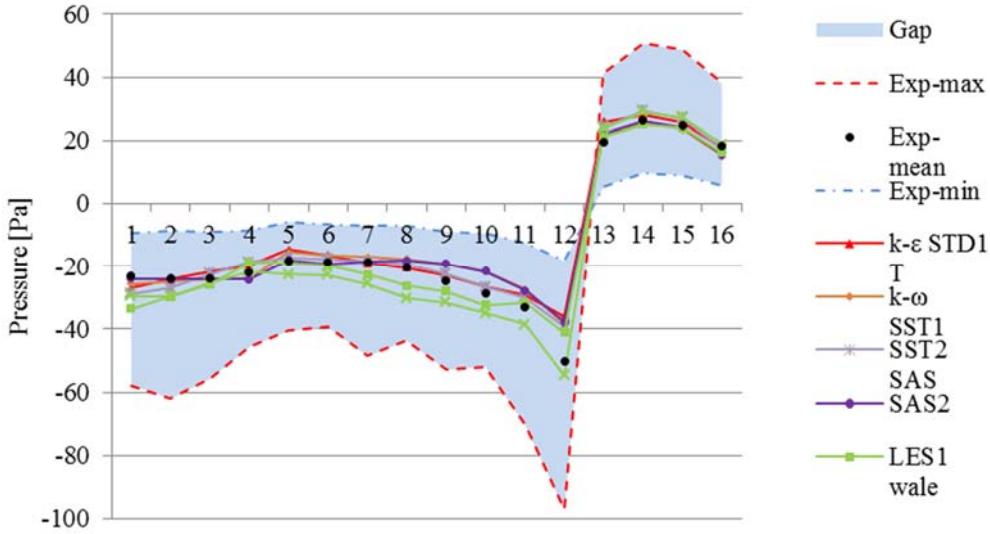

Fig. 4: Comparison of different turbulence models, elevation +0.015m, model M1

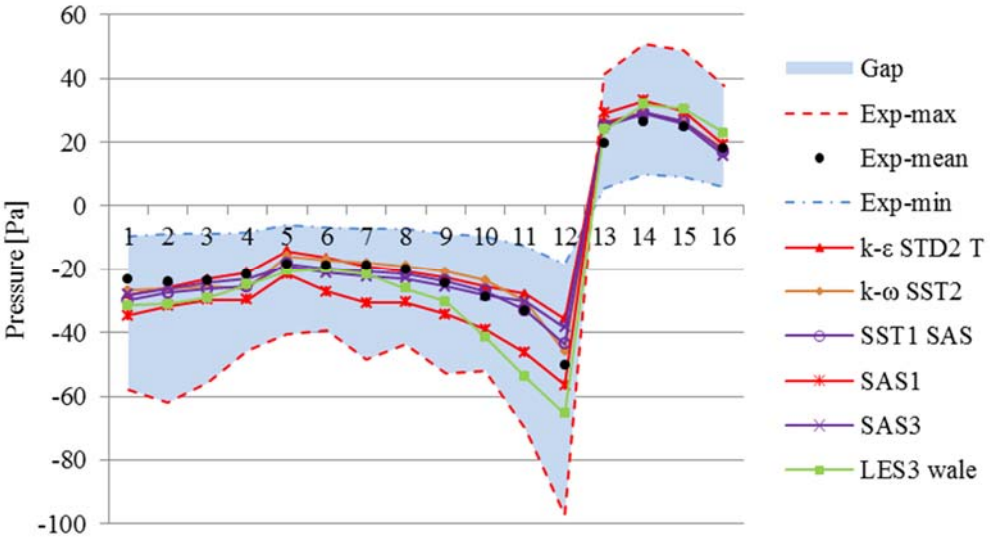

Fig. 5: Comparison of different turbulence models, elevation +0.015m, model M2

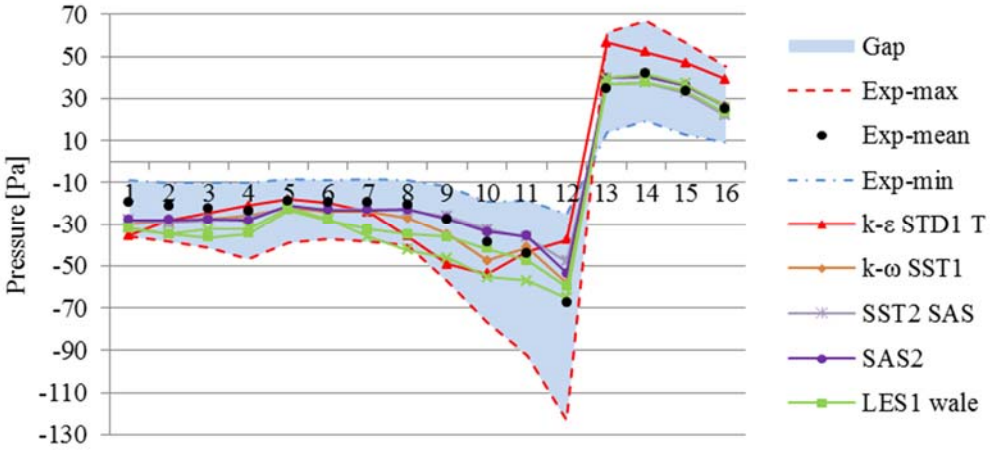

Fig. 6: Comparison of different turbulence models, elevation +0.136m, model M1

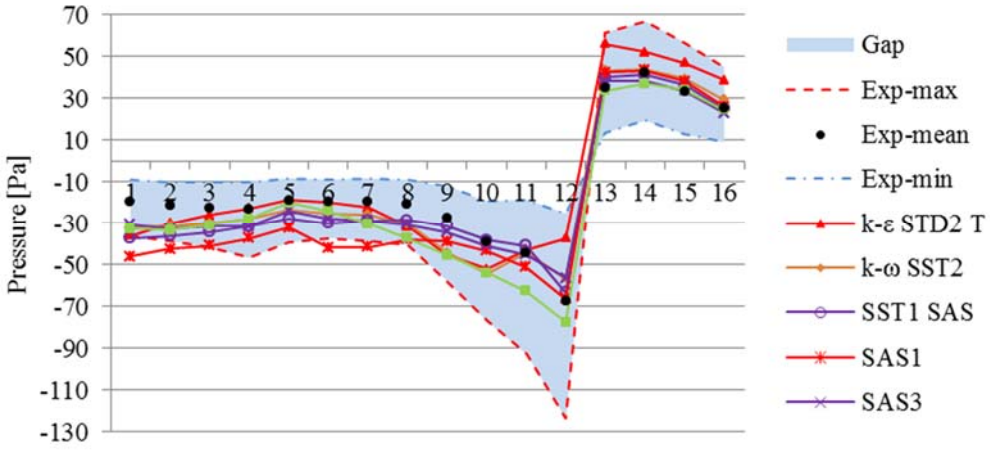

Fig. 7: Comparison of different turbulence models, elevation +0.136m, model M2

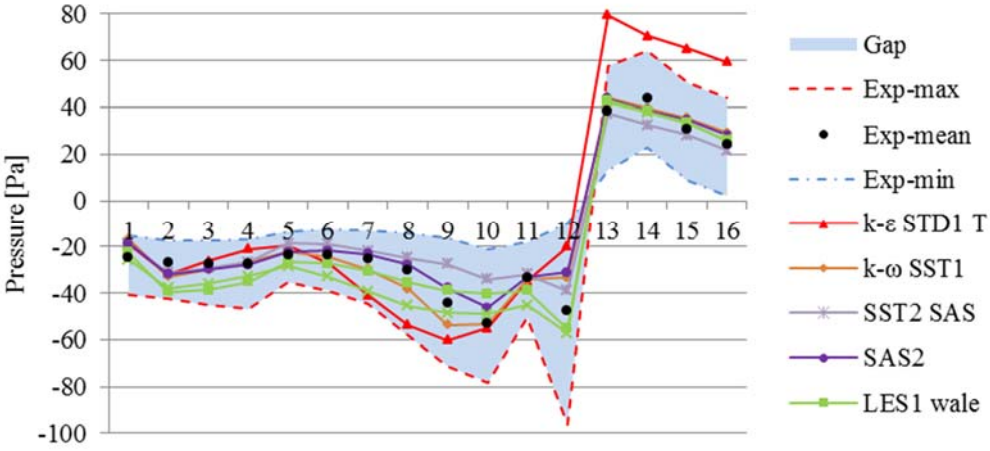

Fig. 8: Comparison of different turbulence models, elevation +0.258m, model M1

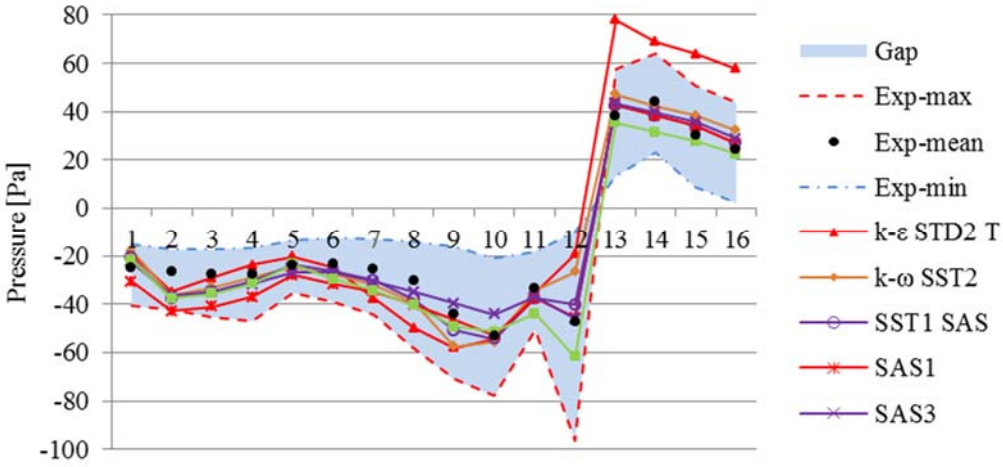

Fig. 9: Comparison of different turbulence models, elevation +0.258m, model M2

Results from experiment are shown as shaded area "Gap", mean value of pressure is represented by black dots. Two different models are compared M1 with 354593 polyhedral cells and M2 with 700200 polyhedral cells. Transient simulation was chosen because of its possibility of averaging results from several iterations, what basically means that the influence or effects of turbulence is been slowly removed.

Absolute values of averaged errors between experiment measurement and CFD simulations can be seen in Tab.1. Here the errors represent the percentage differences between experiment value and CFD value in each point, which have been averaged for objects windward face (points 13 to 16), leeward face (points 1 to 4) and quarter-circle face (points 5 to 12).

Tab. 1: Averaged errors [%] in pressure values

Location\Model	k-ε STD1 T	k-ω SST1	SST1 SAS	SAS2	LES1	LES2
Windward Face	54.26	17.16	15.24	9.32	7.71	9.46
Leeward Face	20.15	17.89	34.67	15.91	38.07	30.19
Quarter-Circle Face	26.48	10.52	10.57	12.93	20.99	34.99
All Points	31.84	15.68	18.93	12.77	21.94	27.40
Location\Model	k-ε STD2 T	k-ω SST2	SST2 SAS	SAS1	SAS3	LES3
Windward Face	53.20	16.52	10.43	15.54	11.62	13.65
Leeward Face	21.11	25.53	19.34	57.50	26.16	31.86
Quarter-Circle Face	23.17	20.75	15.27	37.71	16.94	30.14
All Points	30.16	20.89	15.08	37.11	17.92	26.45

Final numbers of iterations for each turbulence model are shown in Tab.2, these were different from expected number of iterations based on Steps multiplied by Iterations.

Tab. 2: Residuals and convergence

Curve Mark	Time [s]	Steps x Iterations	Num. of Iterations	Abs. Criteria: Continuity	Time Step
k-ε STD1 T	1	4 000	1551	7.6533e-05	0.005
k-ε STD2 T	1	4 000	1787	7.6504e-05	0.005
k-ω SST1	1	3 000	1744	7.6498e-05	0.01
k-ω SST2	1	6 000	1201	2.9532e-05	0.005
SST1 SAS	1	15 000	3654	8.6054e-05	0.001
SST2 SAS	1	15 000	10550	9.5301e-05	0.002
SAS1	0.3	12 000	4792	7.8240e-05	0.0005
SAS2	1	15 000	3685	9.5531e-05	0.002
SAS3	1	15 000	11690	9.7329e-05	0.002
LES1	1	15 000	13137	9.7781e-05	0.002
LES2	1	15 000	13231	8.7978e-05	0.002
LES3	0.6705	26 082	20131	7.8754e-05	0.0005

6 CONCLUSION

From presented results, graphs on Fig.4-9 and Tab.1, can be seen that the transient CFD analysis predicts quite similar flow as obtained from experiment. Because of high CPU requirements, were simulations ran with small amount of iterations for time averaging. This had influence on transient results, this is also mention in several works, [11, 12 and 13]. It can be seen on curves that the influence of turbulence was still present and more iterations are preferred. Several authors claiming similar problems in their work [14, 15 and 16] (convergence, CPU needs, time).

Results from model M2 with dense mesh were more accurate, for the cost of more time needed for analyse. Best performed SST turbulence model with dense grid (M2), but SAS turbulence model with no perturbations using grid M1 predicted pressures with less errors. Looks like, that the spectral synthesiser, which is producing turbulent environment inside the whole domain is the reason of higher errors compared to model without it.

ACKNOWLEDGMENT

This contribution is the result of the research supported by Slovak Grant Agency VEGA. Registration number of the project is 1/1039/12.

REFERENCES

[1] WILCOX, D.C. *Turbulence Modeling for CFD*. 3rd edition. La Canada CA: DCW Industries, Inc. 2006. DOI: 10.1017/S0022112095211388.

[2] WILCOX, D.C. Multiscale model for turbulent flows. In: *AIAA 24th Aerospace Sciences Meeting. American Institute of Aeronautics and Astronautics*, 1986. ISBN: 978-1-84821-001-1.

[3] WILCOX, D.C. Formulation of the k-omega Turbulence Model Revisited. In: *AIAA Journal*, Vol. 46, No. 11, pp. 2823-2838, 2008. DOI: 10.2514/1.36541.

[4] MENTER, F.R. Zonal two-equation k-ω turbulence model for aerodynamic flows. In: *AIAA Paper 1993-2906*. Florida: Orlando, 1993. DOI: 10.2514/6.1993-2906.

[5] MENTER, F.R. Two-equation eddy-viscosity turbulence models for engineering applications. In: *AIAA-Journal*, Vol. 32, No. 8, 1994, pp. 1598-1605. DOI: 10.2514/3.12149.

[6] MENTER, F.R., LANGTRY, R.B., LIKKI, S.R., SUZEN, Y.B., HUANG, P.G., and VÖLKER, S. A Correlation based Transition Model using Local Variables Part 1- Model Formulation. In: *ASME-GT2004-53452*, ASME TURBO EXPO, 2004, Austria: Vienna. DOI: 10.1115/1.2184352.

[7] LANGTRY, R.B., MENTER, F.R., LIKKI, S.R., SUZEN, Y.B., HUANG, P.G., and VÖLKER, S. A Correlation based Transition Model using Local Variables Part 2 - Test Cases and Industrial Applications. In: *ASME-GT2004-53454*, ASME TURBO EXPO, 2004, Austria: Vienna. DOI:10.1115/1.2184353.

[8] LANGTRY, R.B., MENTER, F.R. Transition Modeling for General CFD Applications in Aeronautics. In: *AIAA Paper 2005-522*, Vol. 77, Issue 1-4, 2005, pp. 277-303. DOI: 10.1007/s10494-006-9047-1.

[9] NICOUD, F. AND DUCROS, F. Subgrid-Scale Stress Modelling Based on the Square of the Velocity Gradient Tensor Flow. In: *Turbulence and Combustion.* Vol. 62, Issue 3, 1999, pp. 183–200. DOI: 10.1023/A:1009995426001.

[10] HUBOVA, O., KONECNA, L., OLEKSAKOVA I. Experimental and Numerical Determination of Wind Pressure Distribution on an Object with Atypical Form. In: *Applied Mechanics and Materials*, Vol. 769, 2015, pp. 185-192.ISBN: 978-3-03835-485-7.

[11] TARABA, B., MICHALEC, Z., MICHALCOVA, V., BOJKO, M., KOZUBKOVA, M. CFD simulations of the effect of wind on the spontaneous heating of coal stockpiles. In: *Fuel.* NL: Elsevier Amsterdam, 2014, Vol. 118, pp. 107-112. DOI:10.1016/j.fuel.2013.10.064.

[12] J. KALA, M. BAJER, J. BARNAT, R. KARASEK, O. KRATOCHVIL, A. PECHAL, *Determination of the air flow induced cyclic stressing of a bridge structure.* In: EUROSTEEL 2011, Budapest, Hungary, 2011, pp. 1353-1359. ISBN: 978-92-9147-103-4.

[13] BLEJCHAŘ, T., MICHALCOVÁ, V. *Proudění v mezní vrstvě atmosféry v okolí uhelné skládky – efekt směru vzduchu na samovzněcování (Flow in Atmospheric Boundary Layer in the Surrounding of Coal Stockpile – Effect of Air Direction on Spontaneous Ignition).* In: *Archivum Combustionis*, Polska akademia nauk (PAN), 2010, s. 115-124. ISSN 0808-419X.

[14] BLEJCHAŘ, T. CFD simulace volného smykového proudění a porovnání výsledků s měřením (CFD Simulation of Jet Flow and Comparison with Measurement). In: *Sborník vědeckých prací Vysoké školy báňské - Technické univerzity Ostrava.* Řada strojní, Vysoká škola báňská - Technická univerzita Ostrava, 2010, pp. 1-5. ISSN 1210-0471.

[15] BLEJCHAŘ, T., MICHALCOVÁ, V. CFD simulation in boundary layer in coal stockpile surround. *Sborník vědeckých prací Vysoké školy báňské - Technické univerzity Ostrava.* Řada strojní, Vysoká škola báňská - Technická univerzita Ostrava, 2010, s. 9-14. ISSN 1210-0471.

[16] BLEJCHAŘ, T. CFD model redukce emisí NOx metodou SNCR (CFD Model of NOX Reduction by SNCR Method). *Sborník vědeckých prací Vysoké školy báňské - Technické univerzity Ostrava.* Řada strojní, Vysoká škola báňská - Technická univerzita Ostrava, 2009, s. 1-6. ISSN 1210-0471.

Reviewers:

Prof. Ing. Sergeii Kuznetsov, DrSc., ÚTAM AV ČR, v. v. i., Prague, Czech Republic.

Ing. Vladimíra Michalcová, Ph.D., Department of Structural Mechanics, Faculty of Civil Engineering, VŠB – Technical University of Ostrava., Czech Republic.